JOURNAL OF
HYDRO-METEOROLOGY

Research Article

Temporal change of Son Island in Bassac River, Can Tho city, Vietnam by remote sensing

Tran Minh Doan[1], and Dinh Van Duy[2]*

[1] Master student, Faculty of Water Resource Engineering, College of Engineering, Can Tho University; doanm4222017@gstudent.ctu.edu.vn
[2] Faculty of Water Resource Engineering, College of Engineering, Can Tho University; dvduy@ctu.edu.vn

*Corresponding author: dvduy@ctu.edu.vn; Tel.: +84–906975999

Received: 27 July 2024; Accepted: 23 August 2024; Published: 25 December 2024

Abstract: This study utilizes remote sensing to assess the temporal variation of Son Island on the Bassac River, Can Tho City, Vietnam, from 1987 to 2020. The findings indicate that the evolution of Son Island can be divided into two distinct periods. From 1987 to 2013, the island experienced significant migration from upstream to downstream, covering a distance of approximately 250 meters. In contrast, the period from 2013 to 2020 showed stability, with no significant changes in the island's area or center of gravity. Despite noticeable fluctuations in the island's area throughout the observed period, no clear trend was identified, suggesting overall stability. These fluctuations are likely due to errors in image analysis caused by the coarse resolution of Landsat images, tidal effects, and vegetation changes along the island's banks. The migration of Son Island is attributed to erosion at the island's head and deposition at its tail.

Keywords: Son Island; Bassac River; Google earth; Satellite image; Remote sensing; Migration.

1. Introduction

A river island is a land area elevated above the river water level at river branching sections. These islands divide the river section flowing through them into river branches and play a significant role in connecting and influencing the hydraulic, hydrological, morphological, and environmental interactions between the tributaries [1]. River islands have a significant impact on the morphological changes, environment, waterway traffic, and the lives of people on both sides of the river [2, 3, 4–7]. Therefore, research on river islands has been widely conducted around the world [8–12]. In Vietnam, studies on river engineering mainly focus on riverbank erosion. Although river islands play a crucial role in the river ecosystem and environment, research on river islands in Vietnam is still very limited. Particularly in the Vietnamese Mekong Delta (VMD), notable research on river islands includes the River Channel Improvement [13], analysis of factors affecting the change in the area of Long Khanh island, Hong Ngu district, Dong Thap province [14]. Most previous studies only analyzed riverbank erosion, and islands were only mentioned as part of studies on riverbank erosion in the two main river systems, Mekong River and Bassac River, such as applying the Google Earth Engine (GEE) cloud computing platform in monitoring shoreline changes in the VMD region [15]; applying remote sensing and GIS technology to monitor shoreline changes and assess the erosion situation on the Mekong river systems from 1989 to 2017 [16]; and the study on the causes of increased riverbank erosion in the VMD [17].

As mentioned above, there is a gap in the research on river engineering and management in the VMD, particularly concerning the study of river islands along the Mekong River system. Therefore, this study conducts an analysis of the migration of Son Island, located in Can Tho City, to provide a better understanding of the temporal changes of river islands in the VMD.

Son Island is located in the middle of the Bassac River (across from Co Bac Ferry), in Bui Huu Nghia ward, Binh Thuy district, Can Tho city (Figure 1). The island has a surface area (cultivated area) of 67 hectares [18]. Since 2015, Son Island has become a famous tourist destination in Can Tho City, known for its natural beauty, environment, customs, rituals, and the spirit of mutual support within the community [18, 19].

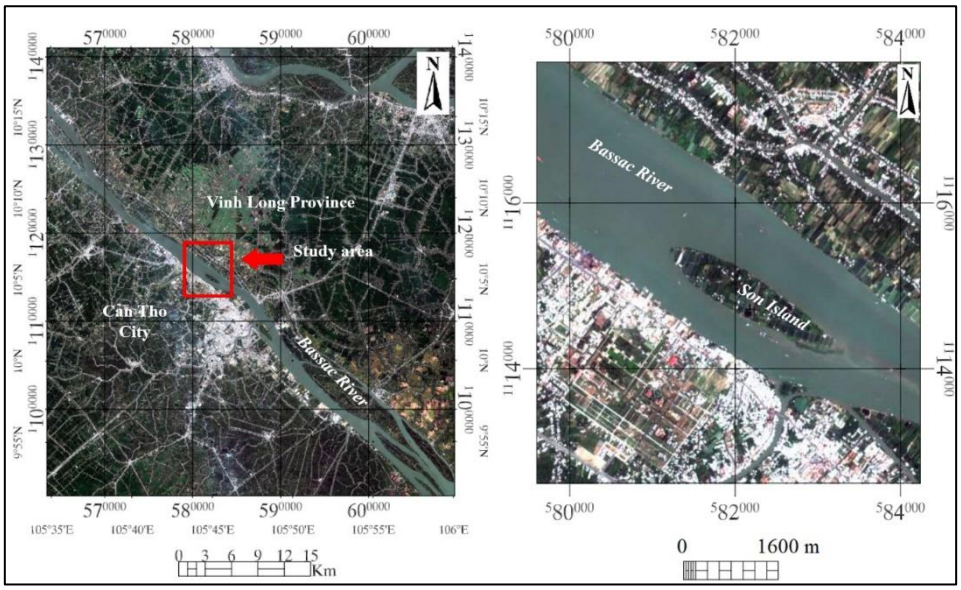

Figure 1. Study area.

2. Materials and Methods

2.1. Satellite image analysis

Landsat images from 1987 to 2020 were used for analysis. Details of the Landsat images are presented in Table 1. In which, there are two types of Landsat images were collected for the analysis with a consistant resolution of 30 m/pixel. The cloud cover varies from 0% to 50%. There are two images collected for each year in the dry and wet seasons. No tidal correction was performed in the image analysis.

Table 1. Information on the Landsat images.

Captured date	Sources	Sensor	Resolution (m)	Cloud cover (%)	Coordinate system
29/12/1987	Landsat 5	TM	30	10.00	UTM
30/01/1988	Landsat 5	TM	30	1.00	UTM
31/12/1988	Landsat 5	TM	30	38.00	UTM
06/04/1989	Landsat 5	TM	30	2.00	UTM
18/12/1989	Landsat 5	TM	30	2.00	UTM
03/01/1990	Landsat 5	TM	30	3.00	UTM
14/05/1991	Landsat 5	TM	30	9.00	UTM
25/01/1992	Landsat 5	TM	30	3.00	UTM
11/01/1993	Landsat 5	TM	30	23.00	UTM
01/04/1993	Landsat 5	TM	30	10.00	UTM
29/12/1993	Landsat 5	TM	30	19.00	UTM
13/10/1994	Landsat 5	TM	30	27.00	UTM
02/02/1995	Landsat 5	TM	30	5.00	UTM

Captured date	Sources	Sensor	Resolution (m)	Cloud cover (%)	Coordinate system
06/03/1995	Landsat 5	TM	30	19.00	UTM
21/02/1996	Landsat 5	TM	30	1.00	UTM
09/04/1996	Landsat 5	TM	30	6.00	UTM
06/01/1997	Landsat 5	TM	30	1.00	UTM
01/07/1997	Landsat 5	TM	30	22.00	UTM
09/01/1998	Landsat 5	TM	30	0.00	UTM
21/06/1999	Landsat 5	TM	30	10.00	UTM
07/07/1999	Landsat 5	TM	30	4.00	UTM
19/03/2000	Landsat 5	TM	30	38.00	UTM
14/11/2000	Landsat 5	TM	30	10.00	UTM
18/02/2001	Landsat 5	TM	30	7.00	UTM
09/05/2001	Landsat 5	TM	30	9.00	UTM
23/11/2003	Landsat 5	TM	30	18.00	UTM
18/06/2004	Landsat 5	TM	30	48.00	UTM
27/12/2004	Landsat 5	TM	30	46.00	UTM
24/08/2005	Landsat 5	TM	30	1.00	UTM
04/03/2006	Landsat 5	TM	30	3.00	UTM
17/12/2006	Landsat 5	TM	30	11.00	UTM
02/01/2007	Landsat 5	TM	30	50.00	UTM
25/03/2008	Landsat 5	TM	30	8.00	UTM
09/12/2009	Landsat 5	TM	30	1.00	UTM
18/05/2010	Landsat 5	TM	30	11.00	UTM
27/06/2013	Landsat 8	OLI_TIRS	30	20.90	UTM
21/01/2014	Landsat 8	OLI_TIRS	30	23.35	UTM
18/09/2014	Landsat 8	OLI_TIRS	30	0.27	UTM
24/01/2015	Landsat 8	OLI_TIRS	30	1.55	UTM
26/12/2015	Landsat 8	OLI_TIRS	30	14.86	UTM
29/01/2017	Landsat 8	OLI_TIRS	30	22.63	UTM
31/10/2018	Landsat 8	OLI_TIRS	30	6.42	UTM
05/12/2019	Landsat 8	OLI_TIRS	30	9.84	UTM
06/01/2020	Landsat 8	OLI_TIRS	30	2.18	UTM
23/02/2020	Landsat 8	OLI_TIRS	30	0.30	UTM

For Landsat imagery, the Normalized Difference Water Index (NDWI) has served as a vital tool for distinguishing water bodies from land. Hence, this study will utilize the NDWI to extract the shoreline between the land area of Son Island and the surrounding water. The application of NDWI follows a specified formula [20]:

$$\mathrm{NDWI} = \frac{\mathrm{GREEN} - \mathrm{NIR}}{\mathrm{GREEN} + \mathrm{NIR}} \quad (1)$$

where GREEN refers to the green light channel and NIR refers to the near-infrared channel. For Landsat 5 satellite images, the GREEN channel corresponds to Band 2 and the NIR channel corresponds to Band 4 [21]. Hence:

$$\mathrm{NDWI} = \frac{\mathrm{Band\,2} - \mathrm{Band\,4}}{\mathrm{Band\,2} + \mathrm{Band\,4}} \quad (2)$$

For Landsat 8, the GREEN component corresponds to channel 3, while the NIR component aligns with channel 5 [22]. Therefore, equation (1) becomes:

$$\mathrm{NDWI} = \frac{\mathrm{Band\,3} - \mathrm{Band\,5}}{\mathrm{Band\,3} + \mathrm{Band\,5}} \quad (3)$$

After applying the NDWI index to the Landsat images, the resulting NDWI images will be classified to convert the shoreline into polygons. These polygons will be imported into AutoCAD to calculate the geometric characteristics of Son Island in plan view, such as area and center of gravity coordinates. Figure 2a shows the NDWI image of Son Island and the classification process, while Figures 2b-2d details the classification process.

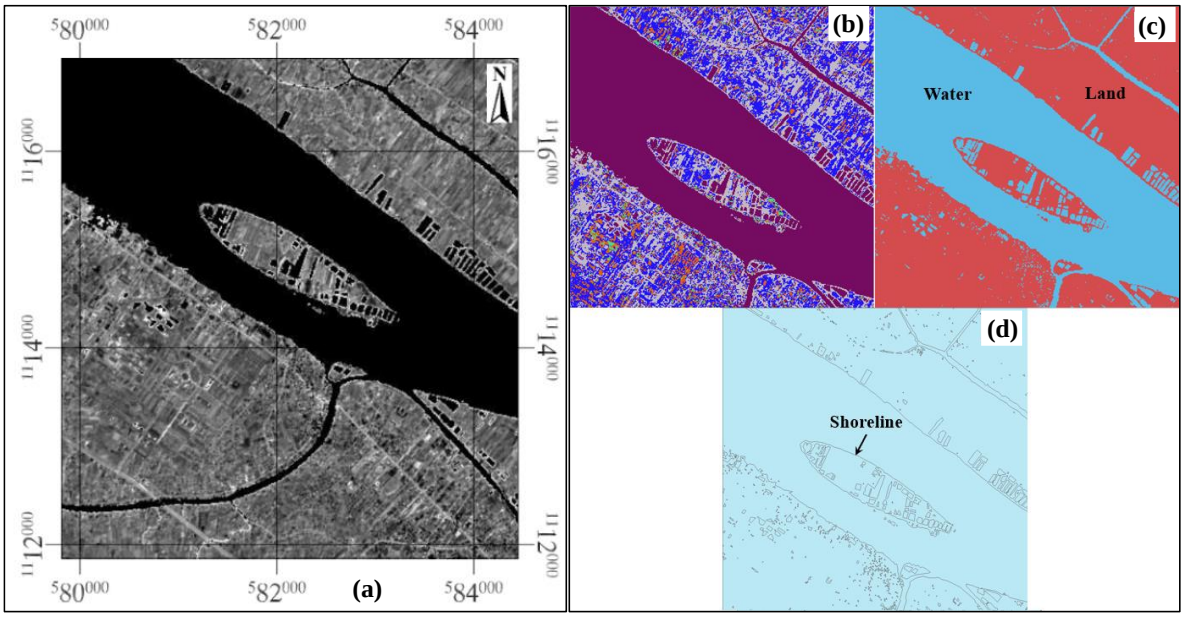

Figure 2. (a) NDWI image of Son Island, (b-d) Classification and shoreline extraction.

2.2. Geometric characteristics of Son Island

In parallel with monitoring the shoreline changes of Son Island, the geometric characteristics of Son Island, such as the center of gravity coordinates and surface area, are also used to analyze the changes of Son Island. The geometric characteristics of Son Island are illustrated in Figure 3.

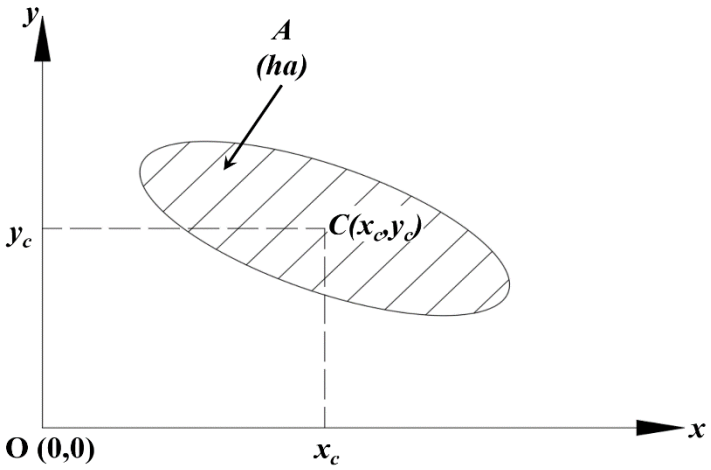

Figure 3. Geometric characteristics of Son Island.

3. Results

3.1. Shoreline changes

Shoreline changes of Son Island from 1987 to 2020 are presented in Figure 4. For readability, only four selected shorelines from 1987, 1995, 2010, and 2020 are shown. As illustrated in the figure, the island migrated approximately 250 meters from 1987 to 2010 due to erosion at the island's head and deposition at its tail. Since 2010, the shoreline of Son Island appears to have stabilized. The development of tourism on Son Island since 2010 may have contributed to this stabilization, as local people have worked to stabilize the riverbank to facilitate tourism.

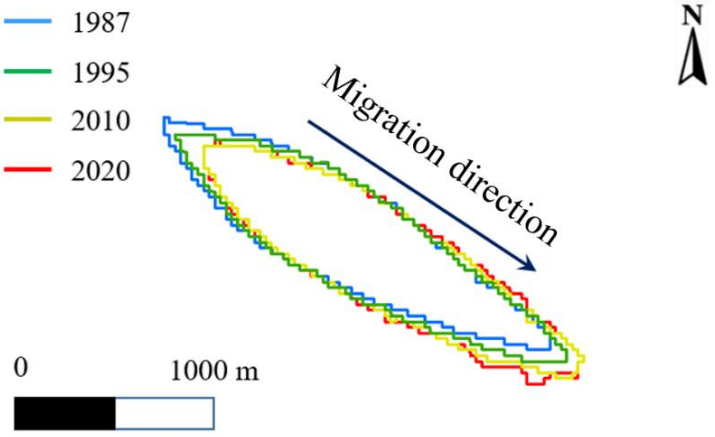

Figure 4. Shoreline changes of Son Island.

3.2. Geometric characteristics of Son Island

The temporal variation of Son Island's area is presented in Figure 5. Although there is significant fluctuation in the area throughout the observed period, there is no clear trend in the variation of the island's area, as indicated by a very small regressor (0.0003). This negligible regressor indicates that the island's area remained stable during the observed period from 1987 to 2020. The significant scatter in the island's area may be a result of errors due to the coarse resolution of the Landsat image, tidal effects, and the appearance/disappearance of vegetation along the riverbanks.

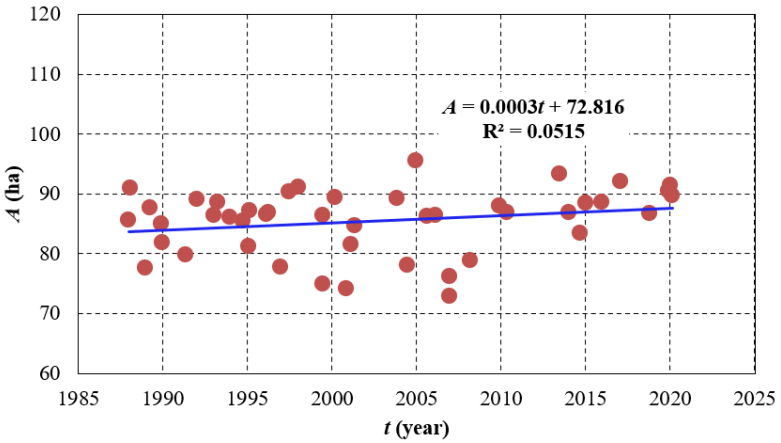

Figure 5. Temporal variation of the Son Island's area.

The figures display the temporal variation of the center of gravity coordinates (x_c and y_c) of Son Island from 1987 to 2020. Figure 6a shows the variation in the x-coordinate (x_c) over time, with blue squares representing the data points and red lines indicating the trend. The first trend line, covering 1987 to approximately 2013, shows a strong positive trend with the equation x_c = 0.024t + 581193 and a high R^2 value of 0.93. From 2013 onwards, the trend line x_c = −0.0003t + 582169 exhibits a near-zero slope and a very low R^2 value of 0.0006, indicating no significant trend. Figure 6b illustrates the variation in the y-coordinate (y_c) over the same period. The first trend line, from 1987 to around 2013, shows a strong negative trend with the equation y_c = −0.0146t + 1E + 06 and an R^2 value of 0.91. Post-2005, the trend line y_c=0.0003t + 1E + 06 has a near-zero slope and an R^2 value of 0.0015, indicating no significant change. These figures suggest that the center of gravity of Son Island shifted significantly in both *x* and *y* directions from 1987 to 2013 but has remained relatively stable since 2013. These results agree well with the shoreline changes mentioned in the previous section.

Table 2. Temporal variation of the center of gravity coordinates (x_c and y_c) of Son Island.

Periods	**1987-2013**		**2013-2020**	
Variables	Regression equation	R^2	Regression equation	R^2
x_c	x_c = 0.024t+581193	0.93	x_c = −0.0003t+582169	0.0006
y_c	y_c = −0.0146t+1E+06	0.91	y_c = 0.0003t+1E+06	0.0015

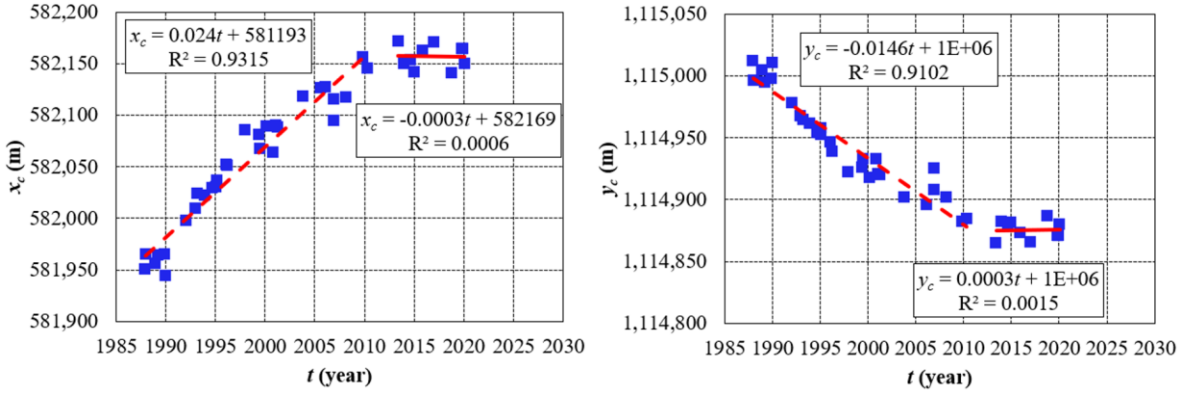

Figure 6. Temporal variation of the Son Island's center of gravity.

4. Conclusions

Remote sensing has been applied to rapidly assess the temporal variation of Son Island on the Bassac River, Can Tho City, Vietnam, from 1987 to 2020. The main findings of this study can be summarized as follows:

- The evolution of Son Island from 1987 to 2020 can be divided into two periods: the first period from 1987 to 2013, during which the island significantly shifted from upstream to downstream by approximately 250 meters; and the second period from 2013 to 2020, which showed the stability of the island with no changes in its area or center of gravity.
- Although there was significant fluctuation in the island's area from 1987 to 2020, there is no obvious trend in the evolution of the island's area, indicating that the island's area remained stable during the observed period. The fluctuation in the island's area can be attributed to errors in image analysis due to the coarse resolution of the Landsat images, tidal effects, and vegetation along the island's banks.
- The migration of Son Island from upstream to downstream is the result of erosion at the island's head and deposition at the island's tail.

Author contribution statement: Developing research ideas: D.V.D.; Process data: processing, manuscript writing: D.V.D., T.M.D.; GIS: D.V.D., T.M.D.; Reviewed and completed the manuscript: D.V.D.

Competing interest statement: The authors declare no conflict of interest.

References

1. Shi, H.; Gao, C.; Dong, C.; Xia, C.; Xu, G. Variation of river islands around a large city along the Yangtze River from satellite remote sensing images. *Sensors* **2017**, *17(10)*, 2213.
2. Liu, X.; Huang, H.; Deng, C. A theoretical investigation of the hydrodynamic conditions for equilibrium island morphology in anabranching rivers. *Adv. Water Sci.* **2014**, *25(4)*, 477–483.
3. Sun, J.; Ding, L.; Li, J.; Qian, H.; Huang, M.; Xu, N. Monitoring Temporal Change of River Islands in the Yangtze River by Remotely Sensed Data. *Water* **2018**, *10(10)*, 1484.
4. Knighton, A.D.; Nanson, G.C. Anastomosis and the continuum of channel pattern. *Earth Surf. Processes Landforms* **1993**, *18(7)*, 613–625.
5. Hooke, J.; Yorke, L. Channel bar dynamics on multi-decadal timescales in an active meandering river. *Earth Surf. Processes Landforms* **2011**, *36(14)*, 1910–1928.
6. Picco, L.; Mao, L.; Rainato, R.; Lenzi, M.A. Medium-term fluvial island evolution in a disturbed gravel-bed river (Piave River, Northeastern Italian Alps). *Geogr. Ann. Ser. A Phys. Geogr.* **2014**, *96(1)*, 83–97.
7. Wu, J.; Fan, M.; Zhang, H.; Shaukat, M.; Best, J.L.; Li, N.; Gao, C. Decadal evolution of fluvial islands and its controlling factors along the lower Yangtze River. *Front. Environ. Sci*. **2024**, *12*, 1388854.
8. Gilvear, D.; Willby, N. Channel dynamics and geomorphic variability as controls on gravel bar vegetation; River Tummel, Scotland. *River Res. Appl.* **2006**, *22(4)*, 457–474.
9. Joeckel, R.; Henebry, G. Channel and island change in the lower Platte River, Eastern Nebraska, USA: 1855–2005. *Geomorphology* **2008**, *102(3-4)*, 407–418.
10. Mani, P.; Kumar, R.; Chatterjee, C. Erosion study of a part of Majuli River-Island using remote sensing data. *J. Indian Soc. Remote Sens*. **2003**, *31*, 12–18.
11. Sadek, N. Island development impacts on the Nile River morphology. *Ain Shams Eng. J.* **2013**, ***4(1)***, 25–41.

12. Wyrick, J.; Klingeman, P. Proposed fluvial island classification scheme and its use for river restoration. *River Res. Appl.* **2011**, *27(7)*, 814–825.
13. Hau, L.P.; Hoang, T.B.; Hung, N.N. River and cannal regulation. Construction Publishing House, Hanoi, 2020, pp. 305.
14. Tu, L.H.; Duy, D.V.; Tri, L.H.; An, N.T.; Minh, H.V.T.; Hong, H.T.C.; Ty, T.V. Analyzing the factors affecting the surface area change of Long Khanh island in Hong Ngu district, Dong Thap province. *VN J. Hydrometeol.* **2021**, *732*, 1–12.
15. Long, V.H.; Giang, N.V.; Hoanh, T.P.; Hoa, P.V. Applying google earth engine in river bank erosion monitoring – A case study in lower Mekong river. *J. Sci.* **2019**, *16(6)*, 38–49.
16. Diep, N.T.H.; Thanh, L.K.; Vinh, L.T.Q.; Minh, V.Q.; Truong, P.N. Progress of landslide situation along Tien and Hau rivers, Mekong Delta. *Can Tho Uni. Sci. J* **2019**, *55*, 125–133.
17. Hoai, H.C.; Bay, N.T.; Khoi, D.N.; Nga, T.N.Q. Analyzing the causes producing the rapidity of river Bank erosion in mekong delta. *VN J. Hydrometeol.* **2019**, *703*, 42–50.
18. Van, T.T.T.; An, N.D.; Nga, T.H.T. Women and rural tourism in the integration context–case study in Con Son, Can Tho. *VNUHCM J. Social Sci. Humanit.* **2020**, *4(4)*, 638–646.
19. Dũ, V.T.; Phương, L.V. Community-based tourism activities in Con Son Island (Mekong Delta- Vietnam) with the issue of preserving cultural and natural values before changes. *Migr. Lett.* **2024**, *21(4)*, 1371–1380.
20. McFeeters, S.K. The use of the normalized difference water index (NDWI) in the delineation of open water features. *Int. J. Remote Sens.* **1996**, *17(7)*, 1425–1432.
21. Ji, L.; Zhang, L.; Wylie, B. Analysis of dynamic thresholds for the normalized difference water index. *Photogramm. Eng. Remote Sens.* **2009**, *75(11)*, 1307–1317.
22. Loveland, T.R.; Irons, J.R. Landsat 8: The plans, the reality, and the legacy. *Remote Sens. Environ.* **2016**, *185*, 1–6.